CONTROL OF FLOW OVER A BLUFF BODY

Haecheon Choi
School of Mechanical and Aerospace Engineering,
Seoul National University
Seoul 151-744, Korea
choi@snu.ac.kr

ABSTRACT

In this paper, we present our recent research activities on control of flow over a bluff body such as a circular cylinder, a two-dimensional bluff body with a blunt trailing edge and a sphere. First, we introduce a three-dimensional forcing applied to a two-dimensional bluff body and show that it significantly changes vortical structures in the wake and reduces mean drag and lift fluctuations. Second, by providing an appropriate active or passive control to a separating shear layer, one can destabilize the shear layer and reattach the flow on the surface before main separation, which delays main separation and decreases drag. Finally, we apply three-different active control methods based on control theories (i.e. linear proportional feedback control, suboptimal feedback control, and active open-loop control using surrogate management framework) to flow over a sphere and show that they successfully reduce the lift fluctuations.

INTRODUCTION

The flow over a bluff body is a common occurrence associated with fluid flowing over an obstacle or with the movement of a natural or an artificial body. Evident examples are the flows past an airplane, a submarine and an automobile, and wind blowing past a bridge and a high-rise building. At much low Reynolds numbers, the flow over a bluff body is highly viscous and the force exerted on the body is mainly attributed to the skin friction. However, when the Reynolds number exceeds a critical value, vortex shedding occurs in the wake, resulting in a significant pressure drop on the rear surface of the body. This vortex shedding occurs over a wide range of Reynolds numbers, causing serious structural vibrations, acoustic noise and resonance, enhanced mixing, and significant increases in the mean drag and the lift fluctuations. Therefore, the effective control of vortex shedding is important in engineering applications.

Efforts have been made to alter and suppress vortex shedding (see the reviews by Zdravkovich (1981), Oertel (1990), Griffin & Hall (1991) and Choi et al. (2008) for these research activities). In the past, many passive and active open-loop control methods were introduced to control vortex shedding behind a two-dimensional bluff body such as a circular cylinder and a two-dimensional blunt-based bluff body. Examples are the endplate, splitter plate, geometric modification in the trailing edge, base bleed, oscillation in line with the incident flow, and rotary oscillation. These control methods are passive or active open-loop in the sense that there is no power input or no feedback sensor, respectively.

Many attempts have been also made to improve the control efficiency and effectiveness using active feedback control methods with the advent of micro-electro-mechanical-system, development of control theory, and fast growth of computer power. The merit of this approach is to obtain the information of the response of flow system to the actuation, and to use it to obtain better control performance than that from the passive or active open-loop control method.

The purpose of this study is to develop effective methods for the control of flow over a bluff body. Three different control approaches are considered. First, we apply a three-dimensional forcing to a two-dimensional bluff body. Second, we provide an appropriate active or passive control to a separating shear layer for its destabilization. Third, we apply active control methods based on control theories (i.e. linear proportional feedback control, suboptimal feedback control, and active open-loop control using surrogate management framework) to flow over a sphere. For the shapes of bluff bodies, we consider a circular cylinder, a two-dimensional bluff body with a blunt trailing edge, and a sphere. The circular cylinder and sphere are the representative two- and three-dimensional bluff bodies, respectively, and their separation points change depending on the Reynolds number. On the other hand, in the case of two-dimensional blunt-based bluff body, the separation is fixed at the trailing edge and hence the flow suddenly changes at the trailing edge from a boundary-layer flow to wake, which is quite different from the cases of circular cylinder and sphere. Therefore, different control strategies may have to be developed when the body shapes are different. A part of the present paper is excerpted from a recent review paper of Choi et al. (2008).

THREE-DIMENSIONAL FORCING FOR TWO-DIMENSIONAL BLUFF BODY

In this section, we provide passive and active open-loop controls varying along the spanwise (or azimuthal) direction, called three-dimensional forcing, to control nominally two-dimensional wake.

Passive control

Examples of three-dimensional geometric modification are the helical strake, segmented trailing edge, wavy trailing edge on a blunt-based model, spanwise waviness to front stagnation face of a rectangular cylinder, circular cylinder with a sinusoidal axis, and circular cylinder with hemispherical bumps (see Choi et al. (2008) and references therein for more details).

We propose a small-size tab, mounted on a part of the upper and lower trailing edges of a two-dimensional bluff body (Fig. 1a; Park et al., 2006), for effectively attenuating vortex shedding and reducing drag. We perform a parametric study by varying the height (l_y) and width (l_z) of the tab and the spanwise spacing between the adjacent tabs (λ). Drag is decreased (or the base pressure is increased) by attaching this simple device at the trailing edge (see Fig.

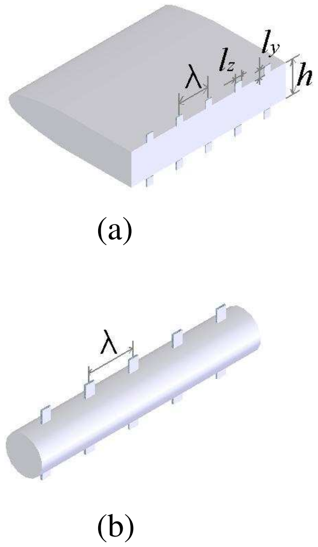

Figure 1: Three-dimensional forcing by tabs: (a) two-dimensional model vehicle; (b) circular cylinder.

2). The optimal configuration of tabs produces about 33% increase in the base pressure. Owing to the tabs, the vortices shed from the upper and lower trailing edges loose their two-dimensional nature and the vortex dislocation occurs. The vortex shedding completely disappears right behind the bluff body but occurs weakly at farther downstream locations (Fig. 3). Since the main mechanism of drag reduction by the tab is to introduce the spanwise phase mismatch in the vortex shedding process and thus to break the nominally two-dimensional nature of vortex shedding, this passive device should work for other two-dimensional bluff bodies such as the circular cylinder.

Therefore, we apply this tab to flow over a circular cylinder at $Re = 100$ (Fig. 1b). The tab located near the separation point reduces drag on a circular cylinder and attenuates the vortex shedding in the wake (Fig. 4). The optimal spanwise spacing between the adjacent tabs is similar to that in Darekar & Sherwin (2001).

However, for three-dimensional bluff bodies such as the sphere or some transportation vehicles, the vortical structures are essentially three dimensional (Yun et al., 2006). In this case, the three-dimensional geometric modifications described above may not produce any drag reduction because they promote three-dimensional vortical activities in the wake. Our preliminary study about flow over a three-dimensional body with the tab did not produce any drag reduction. Therefore, some other types of passive device should be developed for reduction of drag on a three-dimensional body.

Active open-loop control

When a time-periodic open-loop forcing is applied, vortex shedding in the wake is in general locked in phase to the forcing (Blevins, 1990), and consequently the forcing strengthens vortex shedding and increases the mean drag and the lift fluctuations. There are a few successful active open-loop controls that attenuate vortex shedding and reduce drag. One example is the high-frequency rotation of the circular cylinder by Tokumaru & Dimotakis (1991) and another is the base bleed (Wood, 1964; Bearman, 1967). Although these controls are effective in reducing drag, their efficiencies are not so high.

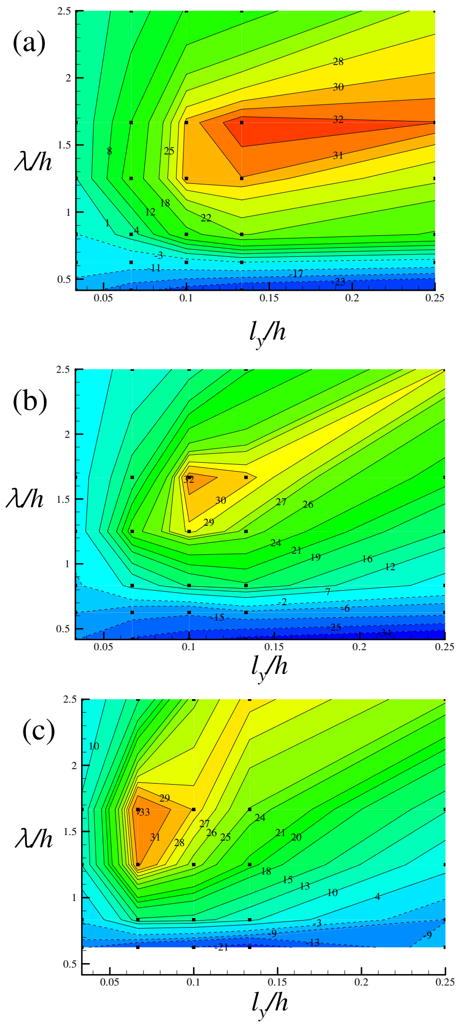

Figure 2: Contours of $\Delta\bar{C}_{pb}$ with respect to λ and l_y at $Re = u_\infty h/\nu = 40,000$: (a) $l_z/h = 0.1$; (b) 0.133; (c) 0.2. $\Delta\bar{C}_{pb} = \left(\bar{C}_{pb}(\text{controlled}) - \bar{C}_{pb}(\text{uncontrolled})\right)/|\bar{C}_{pb}(\text{uncontrolled})| \times 100$, and $\bar{C}_{pb}$ is the mean base-pressure coefficient. From Park et al. (2006).

There are only a few active control methods employing the three-dimensional forcing in the literature. In Kim & Choi (2005), we numerically investigate the effect of the three-dimensional (called 'distributed') forcing on the drag and lift forces on a circular cylinder. The distributed forcing considered is a blowing and suction from the slots located at upper and lower surfaces of the cylinder. The blowing and suction profile from each slot is sinusoidal in the spanwise direction but is steady in time (Fig. 5a):

$$\phi_1(z) = \phi_2(z) = \phi_o \sin(2\pi z/\lambda), \qquad (1)$$

where ϕ_1 and ϕ_2 are the radial velocities at the upper and lower slots, respectively, z is the spanwise direction, ϕ_o is the forcing amplitude, and λ is the forcing wavelength. For all

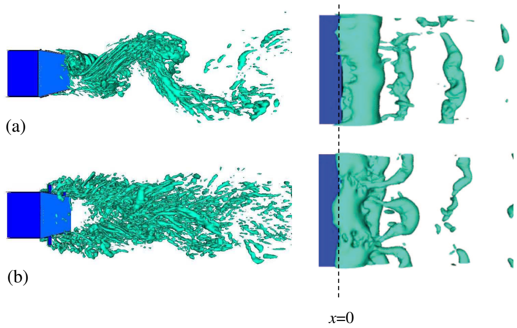

Figure 3: Instantaneous vortical structures in the wake ($Re = u_\infty h/\nu = 4,200$): (a) uncontrolled flow; (b) controlled flow with tabs of $(\lambda/h, l_y/h, l_z/h) = (2, 0.2, 0.2)$. Shown in this figure are the three-dimensional views of vortical structures (left column) and top views of iso-pressure surfaces (right column). From Park et al. (2006).

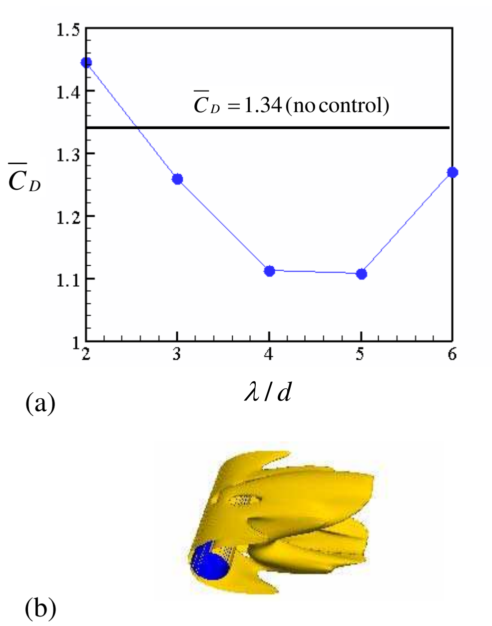

Figure 4: Flow over a circular cylinder with tabs of $(l_y/d, l_z/d) = (0.2, 0.2)$ at $Re = u_\infty d/\nu = 100$: (a) variation of the drag coefficient with the spanwise spacing (λ) of tabs; (b) instantaneous vortical structures in the wake at $\lambda = 4d$. In (b), vortex shedding completely disappears due to the tab.

the Reynolds numbers larger than 46, the distributed forcing attenuates or annihilates the vortex shedding as shown in Figs. 5(b) and (c), and thus significantly reduces the mean drag and the drag and lift fluctuations. Note that, due to the control, vortex shedding completely disappears at $Re = 100$ (Fig. 5b), and nearly disappears in the near wake and reappears weakly in the far wake at $Re = 3900$ (Fig. 5c). The distributed forcing produces the phase mismatch along the spanwise direction in vortex shedding, weakens the strength of vortical structures in the wake, and thus reduces drag.

It is important to note that drag reduction by the distributed forcing is caused by the direct interaction with

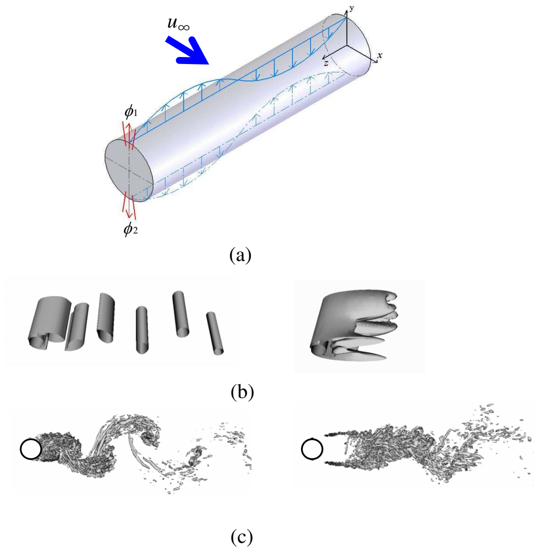

Figure 5: Distributed forcing by Kim & Choi (2005): (a) schematic of the forcing; (b) $Re = 100$ ($\lambda = 5d$); (c) $Re = 3900$ ($\lambda = \pi d$). Shown in (b) and (c) are the instantaneous vortical structures without (left column) and with (right column) control.

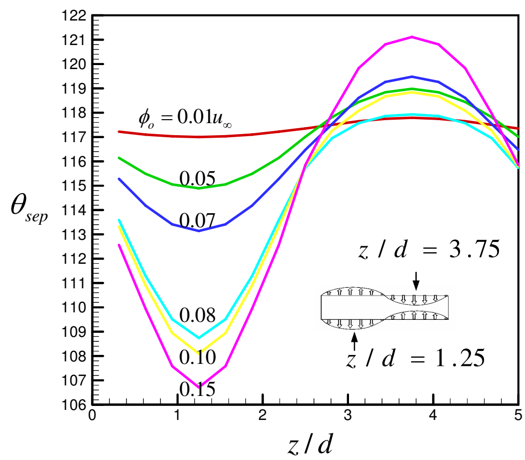

Figure 6: Spanwise variation of the separation angle due to the distributed forcing at Re=100 ($\lambda = 5d$). From Kim & Choi (2005).

vortex shedding, not by the separation delay: as shown in Fig. 6, the separation angle delays at the suction locations but significantly advances at the blowing locations. This fact suggests that the distributed forcing should be also applicable to a body with fixed separation for drag reduction or reduction of lift fluctuations. Thus, we apply the distributed forcing to turbulent flow over a two-dimensional model vehicle having a blunt trailing edge and obtain a significant amount of drag reduction (Kim et al., 2004).

Therefore, the three-dimensional forcing should be applicable to flow over any two-dimensional bluff body, which contains nominally two-dimensional vortex shedding, for drag reduction at various Reynolds numbers.

EARLY SEPARATION AND REATTACHMENT BEFORE

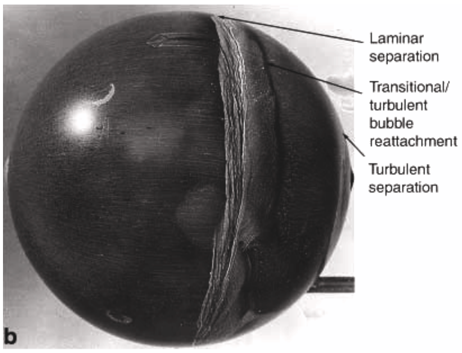

Figure 7: Oil flow pattern on the sphere surface at the critical Reynolds number (Suryanarayana & Prabhu, 2000).

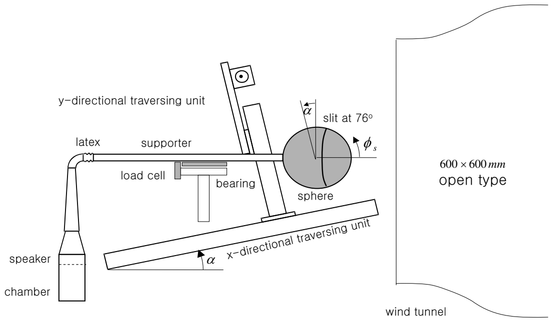

Figure 8: Schematic diagram of the experimental set-up (Jeon et al., 2004).

MAIN SEPARATION

In this section, we consider a sphere which has a movable separation point. For this shape, delay of main separation produces significant drag reduction. To achieve the separation delay, near-wall streamwise momentum should be enhanced near and before the separation point such that it can overcome the adverse pressure gradient formed in the rear part of bluff body. The enhancement of near-wall momentum can be realized by controls either through direct boundary layer transition to turbulence or through early separation and reattachment before main separation. In this study, we show some results from the latter approach.

In the uncontrolled flows over a circular cylinder and a sphere, the drag coefficients rapidly decrease down to about 0.25 and 0.07, respectively, and this phenomenon has been called as the drag crisis (Fage, 1936; Bearman, 1969; Achenbach, 1972; Farell & Blessmann, 1983). The cause of this rapid drag-coefficient reduction is known to be the existence of small separation bubble(s) above the surface (Fig. 7; Suryanarayana & Prabhu, 2000). At the critical Reynolds number, disturbances existing in the boundary layer rapidly grow along the separating shear layer and high momentum fluids in the free-stream are entrained toward the bluff-body surface. This causes the reattachment of the flow (thus forming a separation bubble above the surface) and generates strong near-wall momentum, resulting in the delay of main separation.

We conduct an active control of flow over a sphere for drag reduction using a local time-periodic blowing and suction at subcritical Reynolds numbers, $Re = 6\times10^4 \sim 2\times10^5$

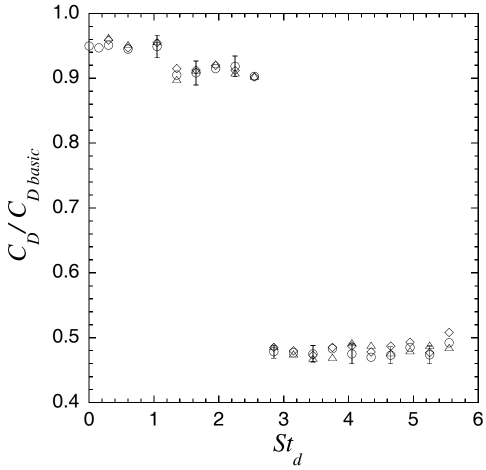

Figure 9: Variations of the drag coefficient with respect to the forcing frequency: ◇, $\phi_o/u_\infty = 0.05$; ○, 0.1; △, 0.15. The vertical bars denote the measurement uncertainty obtained for $\phi_o = 0.1u_\infty$. The drag coefficient at $St_d = fd/u_\infty = 0$ decreases by about 5%, indicating that the flow is a little affected by the blowing/suction slot itself. From Jeon et al. (2004).

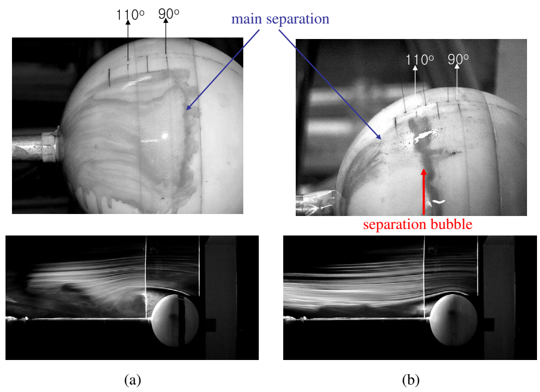

Figure 10: Oil (top) and smoke-wire (bottom) flow visualizations from high frequency forcing (Jeon et al. 2004): (a) without control; (b) with control at $St_d = fd/u_\infty = 4.95$. Here, the flow goes from right to left.

(Fig. 8; Jeon et al., 2004). Significant reductions of the drag coefficient are obtained at the forcing frequencies much higher than the vortex-shedding frequency (Fig. 9). The disturbances from the high frequency forcing rapidly grow along the separating shear layer and high momentum in the free-stream is entrained toward the sphere surface, resulting in the reattachment of the flow (thus forming a separation bubble above the sphere surface; see Fig. 10) and delay of main separation. This mechanism is nearly identical to that observed from the drag crisis.

In Choi et al. (2006), we recently presented a mechanism of drag reduction by dimples on a sphere such as golf-ball dimples by measuring the streamwise velocity above the dimpled surface. It was found that dimples cause local flow separation and trigger the shear layer instability along the separating shear layer, resulting in generation of large turbulence intensity, reattachment to the sphere surface with high momentum near the wall, and delay of main separation

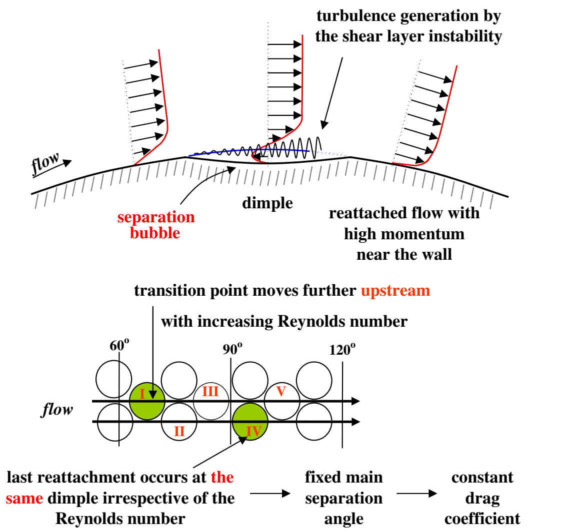

Figure 11: Schematic diagram of drag-reduction mechanism by dimples (Choi et al., 2006).

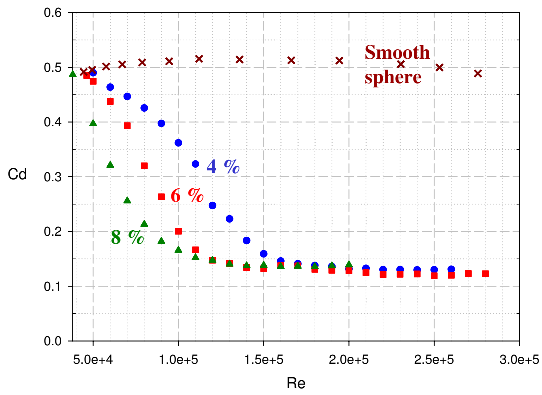

Figure 12: Variations of the drag coefficient on a smooth sphere without (×) and with (solid symbols) free-stream turbulence. Three different turbulence intensities are tested.

(Fig. 11). Again, this mechanism is not very different from that of the drag crisis.

We also investigate the effect of free-stream turbulence on flow over a sphere by installing various types of grids upstream of the sphere. The free-stream turbulence generates small separation bubble above the sphere surface and decreases the critical Reynolds number at which the drag coefficient rapidly decreases (Fig. 12). With further increasing the Reynolds number, the laminar separation point is delayed downstream but the reattachment point closing the separation bubble is fixed at 115°. The main separation point is also fixed at around 130°, resulting in constant drag coefficient after the critical Reynolds number. As the Reynolds number is further increased, the small separation bubble finally disappears but the main separation point is still fixed at 130°. Therefore, the formation, regression and disappearance of the separation bubble are the key to the drag change due to the free-stream turbulence.

The drag on a sphere is also changed by a trip wire located on the sphere surface. Although this behavior is well

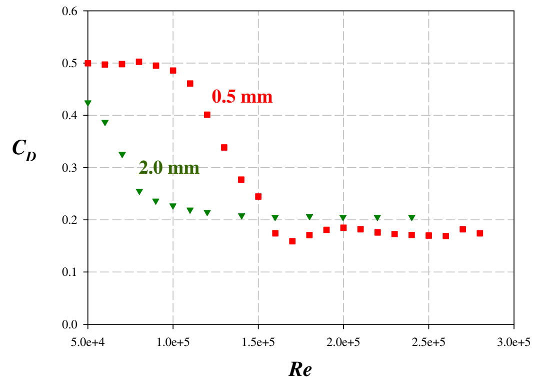

Figure 13: Variations of the drag coefficient on a sphere with a trip wire located at $\phi = 50^o$. Two different trip-wire sizes are tested.

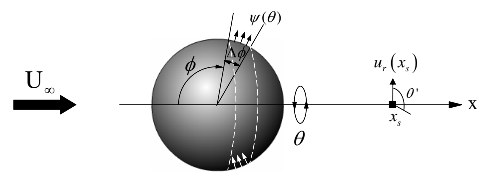

Figure 14: Schematic diagram of the linear proportional control.

known, the flow characteristics have not been clearly presented except that the trip wire promotes transition to turbulence. In our study, we vary the diameter and location of the trip wire, measure the drag, surface pressure and velocity profiles inside the boundary layer, and conduct flow visualization. With a thick trip wire (2mm; $k/d = 1.3{\times}10^{-2}$), a separation bubble is formed right after the trip wire and transition to turbulence occurs there, resulting in main separation delay and drag reduction (Fig. 13). On the other hand, with a thin trip wire (0.5mm; $k/d = 0.3{\times}10^{-2}$), transition to turbulence does not occur at the trip wire but a separation bubble is newly formed at $100^\circ \sim 115^\circ$, which significantly delays the main separation.

Therefore, it is suggested that the generation of a separation bubble before main separation through the separating shear layer instability is an important flow-control strategy for drag reduction on a bluff body having movable separation point such as the sphere and cylinder.

CONTROL THEORIES FOR THREE-DIMENSIONAL BLUFF BODY

Feedback control methods are attractive over the passive and active open-loop controls in that the control input is continuously modified according to the response of the flow system. In this section, we present three successful control methods such as the linear proportional feedback control, suboptimal control, and control based on surrogate management framework.

Linear proportional feedback control

We apply a linear proportional control similar to that proposed by Park et al. (1994). The velocity at the centerline in the wake region is measured for feedback and the control input (blowing/suction) at a part of the sphere sur-

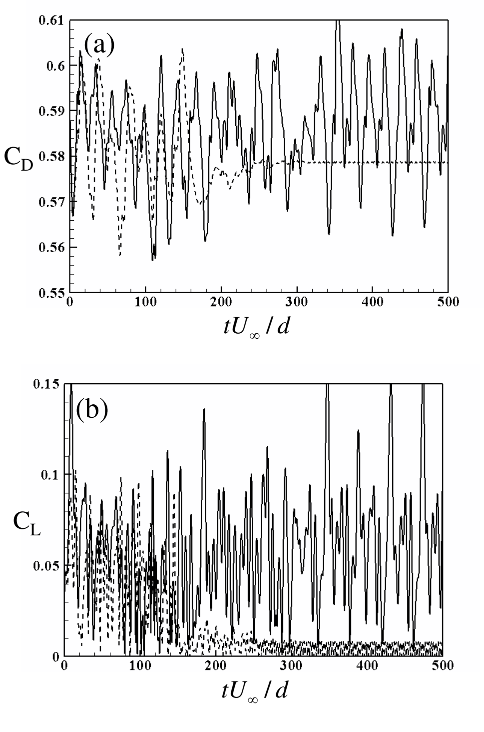

Figure 15: Time histories of the drag and lift coefficients and phase diagram ($Re = 425$): (a) time histories of drag coefficient; (b) time histories of the lift coefficient. ——, Without control; – – –, with control. Shown here is the case of $x_s = 1.2d$ and $\alpha = -0.5$.

face is determined by the measured velocity as follows (Fig. 14):

$$\psi(\theta) = \alpha|u_{r,sensed}|\cos(\theta - \theta') \qquad (2)$$

Here, ψ is the wall-normal actuation velocity (blowing/suction), θ is the azimuthal angle, α is the feedback gain, $u_{r,sensed}$ is the measured radial velocity at the sensing position, x_s, and θ' is the azimuthal angle of measured velocity. Thus, the blowing/suction varies along the azimuthal direction and maximum blowing and suction occur in phase and out of phase to the measured velocity at x_s. Also the amplitude of blowing/suction linearly increases as the measured velocity increases. For the actuation location, we set $\phi = 100^o$ and $\Delta\phi = 20^o$ (see Fig. 14).

We consider $Re = 425$, at which the base flow is unsteady asymmetric. Among various x_s's and α's tested, the most effective sensing position and amplitude are $x_s = 1.2d$ and $\alpha = -0.5$, respectively. Figure 15 shows the time histories of drag and lift coefficients. Here, the lift coefficient is defined as $C_L = \sqrt{C_y^2 + C_z^2}$. The drag and lift fluctuations are significantly reduced by the control. However, the mean drag is almost unchanged.

The present control method strongly depends on the feedback gain α and sensing position x_s. As shown in Fig. 16, when the sensing position or the feedback gain is changed slightly, the drag increases significantly. The fluctuations of lift coefficient are closely related with vortex shedding, and thus it is important to know the sensor location at which the radial velocity along the centerline in the wake is connected with vortex shedding. For this purpose, we define a

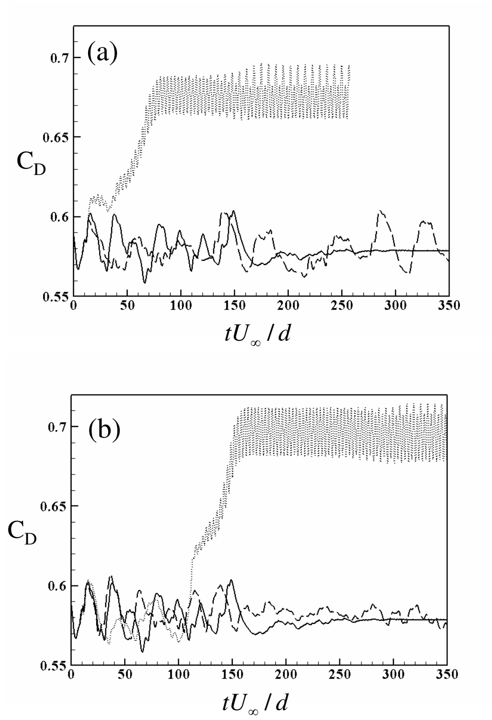

Figure 16: Variations of the drag coefficient with the sensing position and feedback gain ($Re = 425$): (a) – – –, $x_s/d = 1.1$; ——, 1.2; -.-.-, 1.3 ($\alpha = -0.5$); (b) – – –, $\alpha = -0.4$; ——, -0.5; -.-.-, -0.6 ($x_s/d = 1.2$).

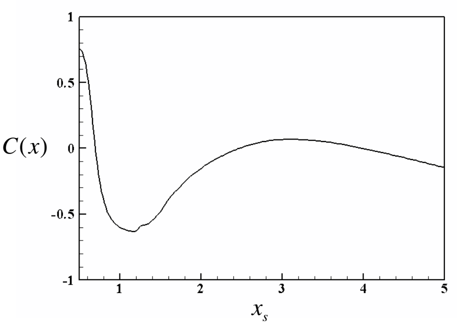

Figure 17: Correlation of the azimuthal angles between the lift and measured velocity ($Re = 425$).

correlation function as follows:

$$C(x) = \frac{1}{T}\int_0^T \cos(\theta_{C_L} - \theta_{u_r})dt, \qquad (3)$$

where θ_{C_L} is the azimuthal angle of lift direction, θ_{u_r} is the azimuthal angle of the direction of measured velocity at the sensing location, and T is the time period of averaging. The value of $C(x)$ becomes 1 when the directions of lift and measured velocity are equal from each other, and -1 when the directions are opposite. Thus, when $|C(x)| \rightarrow 1$, the lift force and measured velocity are well correlated. Figure 17 shows the variation of $C(x)$ with x_s. A strong negative correlation occurs at $x_s = 1.2d$. This location is in good agreement with the x_s location where the control performs well.

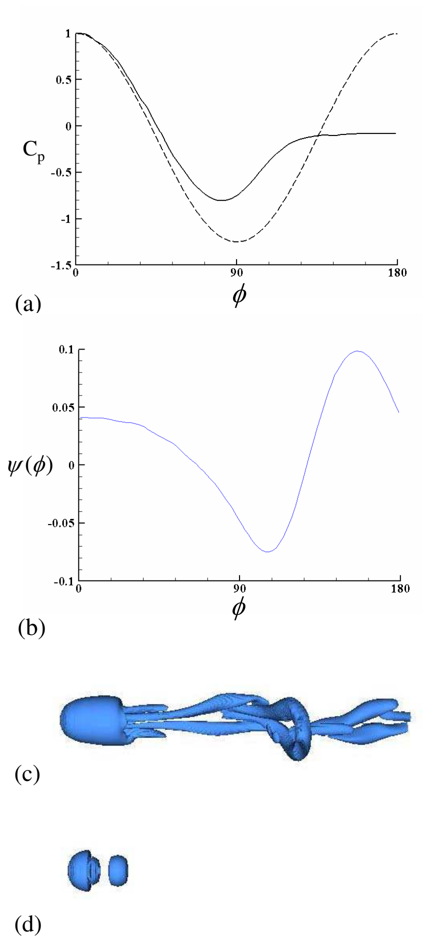

Figure 18: Suboptimal control of flow over a sphere at $Re = 425$: (a) real (solid line) and potential (dashed line) pressure coefficients on the sphere surface; (b) blowing/suction profile along the polar angle; (c) instantaneous vortical structures without control; (d) with control.

Suboptimal control

Optimal control theory has received much attention in flow control. However, the procedure requires the velocity information inside the flow in order to solve the adjoint equations, from which a feedback control input is derived. Therefore, the application of optimal control algorithm to the unsteady three-dimensional Navier-Stokes equations is not practical owing to the complexity of the algorithm. In order to overcome the complexity of the optimal control procedure, Choi et al. (1993) introduced a suboptimal feedback control algorithm, in which the iterations required for a global optimal control were avoided by seeking an optimal condition over a short time period. This control algorithm has been successfully applied to turbulent channel flow (Lee et al., 1998), and flows behind a circular cylinder (Min & Choi, 1999) and a backward-facing step (Choi et al., 1999; Kang & Choi, 2002).

In Min & Choi (1999), we applied a suboptimal feedback control to flow around a circular cylinder at $Re = 100$ and 160. The location of sensors for feedback was limited to the cylinder surface and the control input from actuators was the blowing and suction on the cylinder surface. The cost function to be minimized was the difference between the real and potential pressures on the cylinder surface, and the control input was determined based on the measurement of instantaneous surface pressure. As a result, vortex shedding became weak or disappeared, and the mean drag and drag/lift fluctuations significantly decreased.

We also apply a suboptimal control to flow over a sphere at $Re = 425$. The cost function to be minimized is the difference between the real and potential pressures on the sphere surface (Fig. 18a). The control input is the blowing and suction on the sphere surface and is determined from the measurement of instantaneous surface pressure (Fig. 18b). As a result, we obtain a significant drag reduction through the change in the vortical structures (Figs. 18c and d).

Surrogate Management Framework (SMF)

In the present study, we apply SMF to flow over a sphere to reduce the drag. In the previous sub-section, we applied suboptimal control to the flow over a sphere. As shown in Fig. 18(b), the blowing/suction profile has a wavy shape. Therefore, we adopt sinusoidal blowing/suction as a base function for SMF. The blowing/suction velocity is given as follows:

$$\psi(\phi) = \alpha \left(\psi_{in}(\phi) - \overline{\psi} \right), \tag{4}$$

$$\alpha^2 = \frac{0.01}{\int\int \left(\psi_{in}(\phi) - \overline{\psi} \right)^2 r^2 \sin\phi d\phi d\theta}, \tag{5}$$

$$\psi_{in}(\phi) = A\cos 2\phi - B\sin 2\phi, \tag{6}$$

$$\overline{\psi} = \frac{1}{\pi} \int\int \left(A\cos 2\phi - B\sin 2\phi \right) r^2 \sin\phi d\phi d\theta. \tag{7}$$

Here, r is the radial direction, $0 \le \phi < 180^o$, θ is the azimuthal direction ($0 \le \theta < 360^o$). The parameters A and B are determined through SMF, with the constraints of $-1 < A < 1$ and $-1 < B < 1$. The blowing/suction velocity is homogeneous in the azimuthal direction.

Figure 19 shows the optimal blowing/suction profile obtained from SMF ($A = 0.5, B = -0.3$), which produces about 17% drag reduction. Suction locates at $70^o < \phi < 140^o$, and blowing does elasewhere. Figure 20 shows vortical structures without and with control. As shown, the base flow (unsteady planar-symmetric structure) changes to be steady planar-symmetric with the control.

CONCLUSIONS

In this study, we presented three control methods applied to bluff-body flows. First, we introduced a three-dimensional forcing applied to a two-dimensional bluff body and showed that it significantly changes vortical structures in the wake and reduces mean drag and lift fluctuations. The control directly interacted with flow in the wake rather than through the change in the boundary layer before main separation. Therefore, this control can be applied to flows over two-dimensional bluff bodies with and without fixed separation. Second, by providing an appropriate active or passive control to a separating shear layer, we destabilized the shear layer and reattached the flow on the surface before main separation, which delayed main separation and decreased drag. This phenomenon is quite similar to what happens at the critical Reynolds number without any control. Finally, we applied active control methods based on control theories (i.e. linear proportional feedback control, suboptimal feedback control, and active open-loop control using surrogate management framework) to flow over a sphere. Three controls were all successful in reducing the lift fluctuations.

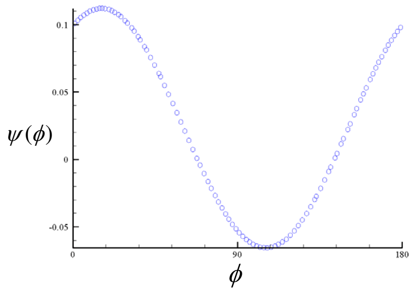

Figure 19: Optimal blowing/suction velocity from SMF.

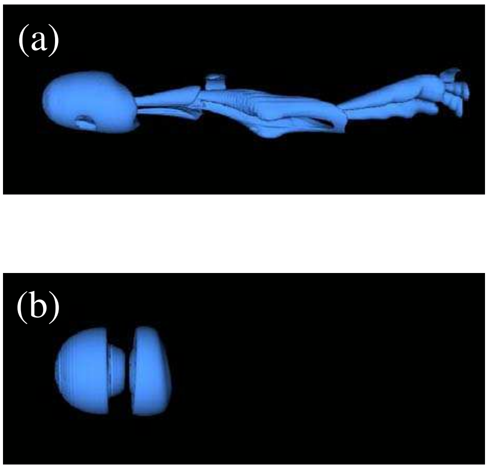

Figure 20: Vortical structures at Re = 300: (a) without control; (b) with SMF control.

ACKNOWLEDGEMENT

The financial support from the National Research Laboratory Program through the Korean Ministry of Science and Technology is gratefully acknowledged.

REFERENCES

Achenbach, E. 1972, "Experiments on the flow past spheres at very high Reynolds numbers", *J. Fluid Mech.*, Vol. 54, pp. 565-575.

Bearman, P. W., 1967, "The effect of base bleed on the flow behind a two-dimensional model with a blunt trailing edge", *Aero. Q.*, Vol. 18, pp. 207-224.

Bearman, P. W., 1969, "On vortex shedding from a circular cylinder in the critical Reynolds number region", *J. Fluid Mech.*, Vol. 37, pp. 577-587.

Blevins, R., 1990, "Flow induced vibration", 2nd Ed., Van Nostrand Reinhold, New York.

Choi, H., Hinze, M., and Kunisch, K., 1999, "Instantaneous control of backward-facing step flows", *Appl. Numer. Math.*, Vol. 31, pp. 133-158.

Choi, H., Jeon, W.-P., and Kim, J., 2008, "Control of flow over a bluff body",*Ann. Rev. Fluid Mech.*, Vol. 40, to appear.

Choi, H., Temam, R., Moin, P., and Kim, J., 1993, "Feedback control for unsteady flow and its application to the stochastic Burgers equation", *J. Fluid Mech.*, Vol. 253, pp. 509-543.

Choi, J., Jeon, W.-P., and Choi, H., 2006, "Mechanism of drag reduction by dimples on a sphere", *Phys. Fluids*, Vol. 18, 041702.

Darekar, R. M., and Sherwin, S. J., 2001, "Flow past a square-section cylinder with a wavy stagnation face", *J. Fluid Mech.*, Vol. 426, pp. 263-295.

Fage, A., 1936, "Experiments on a sphere at critical Reynolds numbers", *Aero. Res. Counc. R & M*, 1766.

Farell, C., and Blessmann, J., 1983, "On critical flow around smooth circular cylinders", *J. Fluid Mech.*, Vol. 136, pp. 375-391.

Griffin, O. M., and Hall, M. S., 1991, "Review-Vortex shedding lock-on and flow control in bluff body wakes", *Trans. ASME: J. Fluids Eng.*, Vol. 113, pp. 526-537.

Jeon, S., Choi, J., Jeon, W.-P., Choi, H., and Park, J., 2004, "Active control of flow over a sphere for drag reduction at a subcritical Reynolds number", *J. Fluid Mech.*, Vol. 517, pp. 113-129.

Kang, S., and Choi, H., 2002, "Suboptimal feedback control of turbulent flow over a backward-facing step", *J. Fluid Mech.*, Vol. 463, pp. 201-227.

Kim, J., and Choi, H., 2005, "Distributed forcing of flow over a circular cylinder", *Phys. Fluids.*, Vol. 17, 033103.

Kim, J., Hahn, S., Kim, J., Lee, D., Choi, J., Jeon, W., and Choi, H., 2004, "Active control of turbulence flow over a model vehicle for drag reduction", *J. Turbulence*, Vol. 5, 019.

Lee, C., Kim, J., and Choi, H., 1998, "Suboptimal control of turbulent channel flow for drag reduction", *J. Fluid Mech.*, Vol. 358, pp. 245-258.

Min, C., and Choi, H., 1999, "Suboptimal feedback control of vortex shedding at low Reynolds numbers", *J. Fluid Mech.*, Vol. 401, pp. 123-156.

Oertel, H., 1990, "Wakes behind blunt bodies", *Ann. Rev. Fluid Mech.*, Vol. 22, pp. 539-564.

Park, D. S., Ladd, D. M., and Hendricks, E. W., 1994, "Feedback control of von Kármán vortex shedding behind a circular cylinder at low Reynolds numbers", *Phys. Fluids*, Vol. 6, pp. 2390-2405.

Park, H., Lee, D., Jeon, W.-P., Hahn, S., Kim, J., Kim, J., Choi, J., and Choi, H., 2006, "Drag reduction in flow over a two-dimensional bluff body with a blunt trailing edge using a new passive device", *J. Fluid Mech.*, Vol. 563, pp. 389-414.

Suryanarayana, G. K., and Prabhu, A., 2000, "Effect of natural ventilation on the boundary layer separation and near-wake vortex shedding characteristics of a sphere", *Exp. Fluids*, Vol. 29, pp. 582-591.

Tokumaru, P. T., and Dimotakis, P. E., 1991, "Rotary oscillatory control of a cylinder wake", *J. Fluid Mech.*, Vol. 224, pp. 77-90.

Wood, C. J., 1964, "The effect of base bleed on a periodic wake", *J. R. Aeronaut. Soc.*, Vol. 68, pp. 477-482.

Yun, G., Kim, D., and Choi, H., 2006, "Vortical structures behind a sphere at subcritical Reynolds numbers", *Phys. Fluids*, Vol. 18, 015102.

Zdravkovich, M. M., 1981, "Review and classification of various aerodynamic and hydrodynamic means for suppressing vortex shedding", *J. Wind Eng. Ind. Aerodyn.*, Vol. 7, pp. 145-189.